

# Coordination Properties of Organoborate Ligands – Steric Hindrance Around the Distal Boron Center Directs the Conformation of the Dialkylbis(imidazolyl)-borate Scaffold

Shiro Hikichi<sup>[a]</sup> Koyu Fujita,<sup>[b]</sup> Yoshitaka Manabe,<sup>[b]</sup> Munetaka Akita,<sup>[b]</sup> Jun Nakazawa,<sup>[a]</sup> and Hidehito Komatsuzaki<sup>[c]</sup>

**Keywords:** Borates / Ligand effects / Nickel / N ligands / C–H⋯M interactions

Alkylmethylbis(imidazolyl)borate ligands,  $[\text{B}(\text{Im}^{N-\text{Me}})_2(\text{alkyl})\text{Me}]^-$  ( $\text{L}^{\text{alkyl}}$ ; alkyl = methyl and *n*-butyl), have been synthesized by nucleophilic substitution from the chloride to the corresponding alkyl derivative on the boron center of the chloroborate precursor. In homoleptic complexes of nickel(II) with  $\text{L}^{\text{alkyl}}$ ,  $[\text{Ni}^{\text{II}}(\text{L}^{\text{alkyl}})_2]$  ( $\mathbf{1}^{\text{alkyl}}$ ), one of the two alkyl groups on the boron atom faces the nickel(II) center to form a C–H⋯M interaction. In the analogous homoleptic nickel(II) complexes of the hydride, phenyl, and methoxy derivatives  $\mathbf{1}^{\text{X}}$  (X = H, Ph, OMe), the boron-attached  $\text{CH}_3$  moieties do not turn towards the metal center. Steric repulsion between the methyl substituent on the imidazolyl ligands and the boron-attached methyl group directs the orientation of the alkyl

groups on  $\text{L}^{\text{alkyl}}$ . In the solution state the molecular structures of  $\mathbf{1}^{\text{alkyl}}$  observed in the solid state are retained. Mixed-ligand complexes,  $[\text{Ni}^{\text{II}}(\text{L}^{\text{alkyl}})(\text{Tp}^{\text{iPr}_2})]$  ( $\mathbf{2}^{\text{alkyl}}$ ), can be synthesized by reaction of  $[\text{Ni}^{\text{II}}(\text{Y})(\text{Tp}^{\text{iPr}_2})]$  (Y = Cl,  $\text{NO}_3$ ) with  $\text{L}^{\text{alkyl}}$  through selective ligand metathesis. In  $\mathbf{2}^{\text{Me}}$ , one methyl group of  $\text{L}^{\text{Me}}$  approaches the nickel center retaining the bent conformation of the two imidazolyl groups. Conversely, the carbon atoms of the boron-attached *n*Bu and Me groups of  $\text{L}^{\text{Bu}}$  are located away from the nickel center, and the orientation of the two imidazolyl groups is almost coplanar in  $\mathbf{2}^{\text{Bu}}$ . The structural characteristics of these nickel(II) complexes demonstrate the flexibility of the dialkylbis(imidazolyl)borate scaffold.

## Introduction

In addition to the metal binding groups of chelating reagents, other ligand components play important roles in the control of the structural and electronic properties of the resulting metal complex. For example, the boron centers of poly(pyrazolyl)borates (“scorpionate” ligands such as  $\text{Tp}^{\text{R}}$  and  $\text{Bp}^{\text{R}}$ ) act as carriers of mononegative charge as four-coordinate borate. In addition, the tetrahedral geometry of the boron center defines the orientation of the substituent groups including the pyrazolyl ligands, which affects the structures of the resulting metal complexes.<sup>[1,2]</sup>

Recently, a variety of organoborate ligand systems including our own bis(imidazolyl)borates have been developed.<sup>[3–8]</sup> The most interesting feature of our organoborate ligand system is the stability of the B–C<sub>imidazolyl</sub> linkage to-

ward hydrolytic decomposition due to the higher covalency of the B–C bond compared to the B–N linkage of poly(pyrazolyl)borates. Therefore, stepwise substitution of the borate core is possible, and various ligands such as the tripodal heteroscorpionate, methylbis(1-methyl-2-imidazolyl)[(3,4,5-substituted)-1-pyrazolyl]borate,<sup>[3]</sup> and a silica-immobilized ligand,<sup>[6]</sup> which is a key component of a catalyst mimicking the active site of nonheme metalloenzymes, can be synthesized by the nucleophilic substitution of the chlorine atom on the boron center in  $[\text{B}(\text{Im}^{N-\text{Me}})_2(\text{Cl})\text{Me}]^-$  ( $\text{L}^{\text{Cl}}$ ).<sup>[4]</sup> The silica-immobilized ligand contains two boron-attached alkyl groups, a methyl group and a linear alkyl chain [i.e., derived from radical coupling of a boron-attached allyl group with a 3-mercaptopropyl group,  $-(\text{CH}_2)_3\text{S}(\text{CH}_2)_3\text{Si}(\text{OR})_3$ ].<sup>[6]</sup> Therefore, an investigation of the coordination behavior of alkylmethylbis(imidazolyl) borate ligands,  $[\text{B}(\text{Im}^{N-\text{Me}})_2(\text{alkyl})\text{Me}]^-$  ( $\text{L}^{\text{alkyl}}$ ), gives us insights into the coordination structure of the active site of our immobilized catalyst. In this study, Me and *n*Bu derivatives of  $\text{L}^{\text{alkyl}}$ ,  $[\text{B}(\text{Im}^{N-\text{Me}})_2\text{Me}_2]^-$  ( $\text{L}^{\text{Me}}$ ) and  $[\text{B}(\text{Im}^{N-\text{Me}})_2(n\text{Bu})\text{Me}]^-$  ( $\text{L}^{\text{Bu}}$ ), have been synthesized by the reaction of  $\text{L}^{\text{Cl}}$  with the corresponding alkylolithium. A series of ligands has been synthesized,  $\text{L}^{\text{alkyl}}$ , and, in turn, a series of nickel(II) complexes has been prepared. The coordination properties of  $\text{L}^{\text{alkyl}}$  and the analogous ligand  $\text{L}^{\text{X}}$ , including the closely related phenyl and hydride derivatives ( $\text{L}^{\text{Ph}}$  and  $\text{L}^{\text{H}}$ ),

[a] Department of Material and Life Chemistry, Kanagawa University, 3-27-1 Rokkakubashi, Kanagawa-ku, Yokohama 221-8686, Japan  
Fax: +81-45-413-9770  
E-mail: hikichi@kanagawa-u.ac.jp

[b] Chemical Resources Laboratory, Tokyo Institute of Technology, 4259 Nagatsuta, Midori-ku, Yokohama 226-8503, Japan

[c] Department of Chemistry and Material Engineering, Ibaraki National College of Technology, 866 Nakane, Hitachinaka, Ibaraki 312-8508, Japan

Supporting information for this article is available on the WWW under <http://dx.doi.org/10.1002/ejic.201000629>.

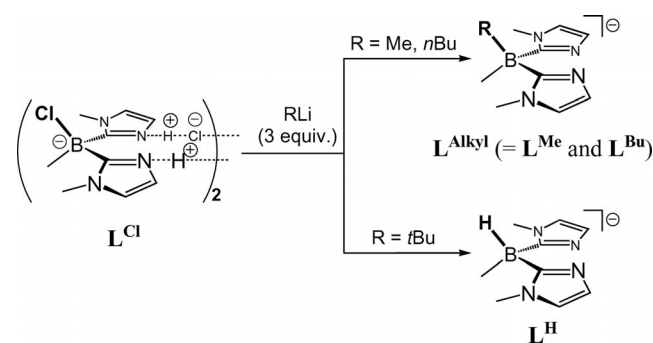
were compared. Steric congestion around the boron center influences the orientation of the metal-binding imidazolyl groups and noncoordinating groups.

## Results and Discussion

### Synthesis of Dialkylbis(*N*-methylimidazolyl)borates $L^{\text{alkyl}}$

As we have reported previously, the reaction of the chlorinated borate compound,  $L^{\text{Cl}}$ , with phenyllithium yields bis(1-methyl-2-imidazolyl)methylphenylborate,  $[B(\text{Im}^{N-\text{Me}})_2\text{Me}(\text{Ph})]^-$  ( $L^{\text{Ph}}$ ).<sup>[4]</sup> The same procedure has been employed to prepare the dialkylbis(1-methyl-2-imidazolyl)borate with methyl ( $L^{\text{Me}}$ ) and *n*-butyl ( $L^{\text{Bu}}$ ) derivatives. The chlorinated precursor,  $L^{\text{Cl}}$ , is formulated as an HCl adduct of the protonated form of chloromethylbis(1-methyl-2-imidazolyl)borate, and therefore, an excess amount (at least three equivalents) of alkylolithium is required to obtain  $L^{\text{alkyl}}$ .

The reaction of  $L^{\text{Cl}}$  with *t*BuLi resulted in the formation of a hydride-containing borate  $[B(\text{Im}^{N-\text{Me}})_2(\text{H})\text{Me}]^-$  ( $L^{\text{H}}$ ) instead of a *t*Bu derivative, i.e.  $[B(\text{Im}^{N-\text{Me}})_2(\text{tBu})\text{Me}]^-$ , as shown in Scheme 1. The IR spectrum of  $L^{\text{H}}$  showed a peak attributed to the B–H vibration at  $2288\text{ cm}^{-1}$  in addition to the B–C<sub>Me</sub> and B–C<sub>imidazolyl</sub> vibrations at around  $1280\text{ cm}^{-1}$ . Due to the coupling with the boron nucleus, the boron-attached H was not detected in the <sup>1</sup>H NMR spectrum. The formation of  $L^{\text{H}}$  might arise from the action of LiH which is generated by pyrolysis of *t*BuLi as well as the bulk and low nucleophilicity of the *t*Bu anion.<sup>[9]</sup>



Scheme 1. Reaction of  $L^{\text{Cl}}$  with alkylolithium.

### Synthesis and Characterization of Homoleptic Nickel(II) Complexes $[\text{Ni}^{\text{II}}(\text{L}^{\text{R}})_2]$

As well as the previously reported  $L^{\text{Ph}}$  and  $\text{Bp}^{\text{R}}$  derivatives,  $L^{\text{alkyl}}$  may behave as a bidentate ligand. In order to clarify the coordination behavior, we examined the reaction of a nickel(II) salt with two equivalents of  $L^{\text{X}}$  ( $\text{X} = \text{alkyl}, \text{H}, \text{Ph}$ ) to obtain homoleptic nickel(II) complexes,  $[\text{Ni}^{\text{II}}(\text{L}^{\text{X}})_2]$  ( $\mathbf{1}^{\text{X}}$ ), containing a stable square planer nickel center. The desired complexes with  $L^{\text{alkyl}}$  ( $\mathbf{1}^{\text{alkyl}}$ ) were obtained and their molecular structures were compared with those of the  $L^{\text{H}}$  and  $L^{\text{Ph}}$  derivatives. The overall molecular structures of the homoleptic complexes,  $\mathbf{1}^{\text{X}}$ , are similar to those of

the nickel(II) complexes with bis(1-pyrazolyl)borates ( $= [B(\text{pz}^{\text{R}})_2\text{R}'_2]^-$ ;  $\text{R}' = \text{H}, \text{alkyl}$ )<sup>[10]</sup> and dimethylbis(2-pyridyl)borate ( $= [B(\text{py})_2\text{Me}_2]^-$ )<sup>[7a]</sup> as shown in Figure 1. The nickel center sits on a crystallographic center of symmetry and is surrounded by the imidazolyl nitrogen atoms in a square-planar arrangement. The six-membered Ni–N–C–

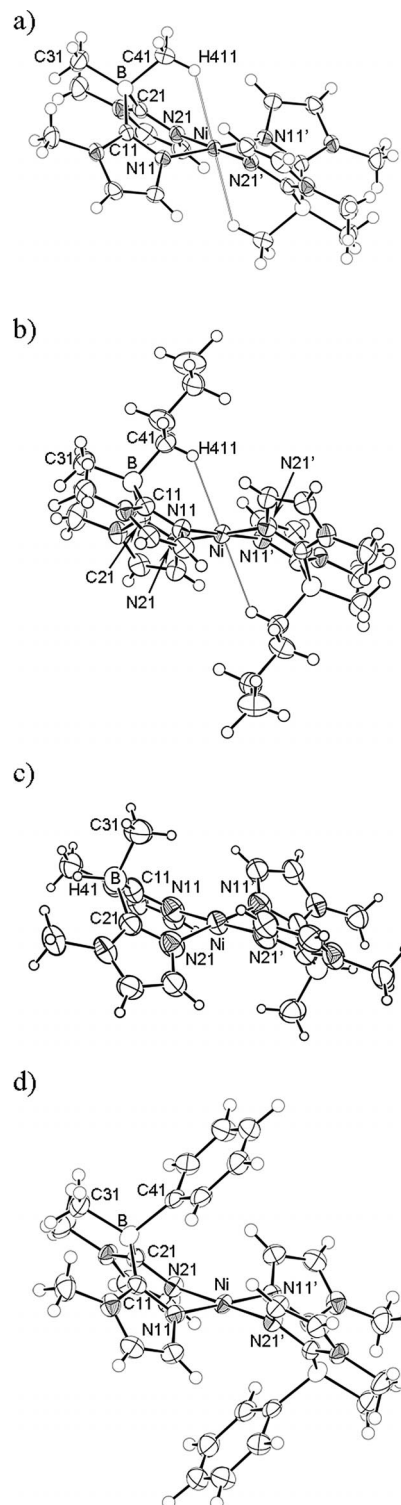


Figure 1. Molecular structures of (a)  $\mathbf{1}^{\text{Me}}$ , (b)  $\mathbf{1}^{\text{Bu}}$ , (c)  $\mathbf{1}^{\text{H}}$ , and (d)  $\mathbf{1}^{\text{Ph}}$ . All diagrams are drawn at 30% probability.

B–C–N ring adopts a boat conformation. However, varying the substituent on the distal boron site influences the coordination environment of the nickel center.

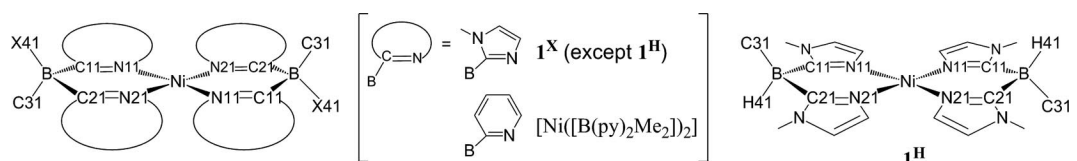
### Structural Characteristics of Dialkyl Ligands Derivatives $\mathbf{1}^{\text{alkyl}}$

The most unique structural property of the  $\mathbf{L}^{\text{alkyl}}$  derivatives of  $\mathbf{1}$  is that the hydrogen atom on the  $\alpha$ -CH group of the boron-attached alkyl group lies in the vicinity of the nickel center. Steric repulsion between the 1-methyl groups on the imidazolyl groups and the boron-bound methyl group leads to a small dihedral angle between the two imidazolyl rings as well as forcing an alkyl (Me or *n*Bu) group to approach the nickel center due to the tetrahedral borate geometry. The shapes of the six-membered Ni–N–C–B–C–N rings exhibit “deep” boat conformations, indicated by somewhat long distances from the nickel and boron centers to the N11–C11–C21–N21 plane consisting of the two imidazolyl ligands. A similar structure has been reported for the nickel(II) complex with dimethylbis(2-pyridyl)borate,  $[\text{Ni}^{\text{II}}(\{\text{B}(\text{py})_2\text{Me}_2\})_2]$ .<sup>[7a]</sup>

Although B–H $\cdots$ M interactions are frequently observed in complexes with poly(pyrazolyl)borate ligands, few examples of agostic C–H $\cdots$ M interactions between the  $\alpha$ -CH of the boron-attached alkyl group and the metal center have been reported for dialkylbis(pyrazolyl)borate complexes.<sup>[2,10–13]</sup> Furthermore, enforced agostic C–H $\cdots$ M interactions are observed in complexes with 1,5-cyclooctanediyl-bis(pyrazolyl)borate (=  $[\text{B}(\text{pz})_2(\text{BBN})]$ ) due to the rigidity and bulk of the boron-attached bicyclic dialkyl moiety.<sup>[13]</sup> In our complexes,  $\mathbf{1}^{\text{alkyl}}$ , the distances between the nickel centers and the  $\alpha$ -CH atom are longer (H411 $\cdots$ Ni; 2.47 Å in  $\mathbf{1}^{\text{Me}}$  and 2.63 Å in  $\mathbf{1}^{\text{Bu}}$ ; see Table 1) than those found in  $[\text{Co}^{\text{II}}(\{\text{B}(\text{pz})_2(\text{BBN})\})_2]$  (H–Co; 2.166 Å).<sup>[13]</sup> Weak C–H $\cdots$ M interactions between square-planer  $d^8$  metal centers and the apical hydrogen atoms of alkyl groups can be classified as “anagostic” interactions in terms of lacking the covalency of a M–H moiety.<sup>[14,15]</sup>

In contrast, the smaller hydride substituent on the boron center is placed in the cleft between the two imidazolyl-attached *N*-methyl groups in  $\mathbf{1}^{\text{H}}$ . Similar structures have been observed in the phenyl-containing ligand complexes  $[\text{Ni}^{\text{II}}(\text{L}^{\text{Ph}})_2]$  ( $\mathbf{1}^{\text{Ph}}$ )<sup>[4]</sup> and  $[\text{Ni}^{\text{II}}(\text{L}^{\text{OMe}})_2]$  ( $\mathbf{1}^{\text{OMe}}$ , where  $\text{L}^{\text{OMe}}$  is bis-

Table 1. Structural parameters for the homoleptic complex  $\mathbf{1}^{\text{X}}$ .



| Compound  | $\mathbf{1}^{\text{Me}}$ | $\mathbf{1}^{\text{Bu}}$ | $\mathbf{1}^{\text{H}}$   | $\mathbf{1}^{\text{Ph}}$ | $\mathbf{1}^{\text{Ph[a]}}$ | $\mathbf{1}^{\text{OMe[b]}}$ | $[\text{Ni}^{\text{II}}(\{\text{B}(\text{py})_2\text{Me}_2\})_2]^{\text{[c]}}$ |
|---|--------------------------|--------------------------|---|--------------------------|-----------------------------|------------------------------|--|
| X   | Me                       | <i>n</i> Bu              | H   | Ph                       | Ph                          | OMe                          | Me   |
| Bond length [Å]   |                          |                          |   |                          |                             |                              |  |
| Ni–N11  | 1.887(3)                 | 1.879(4)                 | 1.888(9)  | 1.887(4)                 | 1.886(2)                    | 1.892(5)                     | 1.906(2)   |
| Ni–N21  | 1.888(3)                 | 1.893(3)                 | 1.911(8)  | 1.880(4)                 | 1.896(2)                    | 1.897(4)                     | 1.902(2)   |
| B–C11   | 1.631(5)                 | 1.647(7)                 | 1.592(16)   | 1.632(8)                 | 1.635(3)                    | 1.650(7)                     | 1.638(4)   |
| B–C21   | 1.637(5)                 | 1.640(7)                 | 1.593(15)   | 1.638(8)                 | 1.633(4)                    | 1.641(8)                     | 1.637(4)   |
| B–C31   | 1.630(5)                 | 1.616(7)                 | 1.642(17)   | 1.617(8)                 | 1.625(4)                    | 1.618(7)                     | 1.623(4)   |
| B–X41   | 1.630(5)                 | 1.643(7)                 | 1.36(14)  | 1.628(8)                 | 1.631(3)                    | 1.477(7)                     | 1.639(4)   |
| Ni $\cdots$ H   | 2.4714                   | 2.6334                   | 3.0898  | –                        | 3.009                       | 2.911                        | 2.343 <sup>[a]</sup>   |
| Distance from the plane N11–C11–C21–N21 (= $\text{N}_2\text{C}_2$ ) [Å]   |                          |                          |   |                          |                             |                              |  |
| $\text{N}_2\text{C}_2\cdots\text{Ni}$   | 0.753(4)                 | 0.757(5)                 | 0.729(14)   | 0.751(6)                 | 0.828(14)                   | 0.736(6)                     | 0.946(1)   |
| $\text{N}_2\text{C}_2\cdots\text{B}$  | 0.710(5)                 | 0.636(7)                 | 0.541(18)   | 0.669(8)                 | 0.484(16)                   | 0.595(8)                     | 0.728(5)   |
| Bond angles [°]   |                          |                          |   |                          |                             |                              |  |
| N11–Ni–N21  | 89.32(12)                | 89.20(16)                | 89.5(4) <sup>[d]</sup>  | 89.17(19)                | 88.48(8)                    | 89.55(17)                    | 89.34(9)   |
| N11–Ni–N21'   | 90.68(12)                | 90.80(16)                | 178.0(4) <sup>[d]</sup><br>90.9(5) <sup>[d]</sup><br>90.2(5) <sup>[d]</sup> | 90.83(19)                | 91.52(8)                    | 90.45(17)                    | 90.66(9)   |
| C11–B–C21   | 100.9(2)                 | 101.8(4)                 | 103.2(10)   | 100.9(4)                 | 103.9(2)                    | 101.8(4)                     | 102.7(2)   |
| C11–B–C31   | 116.1(3)                 | 115.5(4)                 | 110.1(9)  | 116.2(5)                 | 110.1(2)                    | 108.7(4)                     | 111.9(3)   |
| C11–B–X41   | 107.0(3)                 | 106.9(4)                 | 115(4)  | 108.6(4)                 | 109.5(2)                    | 110.5(4)                     | 110.6(2)   |
| C21–B–C31   | 115.9(3)                 | 113.6(4)                 | 112.6(9)  | 116.2(4)                 | 108.0(2)                    | 109.9(4)                     | 111.6(2)   |
| C21–B–X41   | 108.1(3)                 | 108.3(4)                 | 115(4)  | 106.8(4)                 | 111.4(2)                    | 108.7(4)                     | 110.4(2)   |
| C31–B–X41   | 108.2(3)                 | 110.1(4)                 | 101(6)  | 107.6(4)                 | 113.4(2)                    | 116.3(4)                     | 109.5(3)   |
| Dihedral angles between two imidazolyl rings (torsion angles of Z1–B–Ni–Z2; Z1 and Z2 denote the center of the imidazolyl ring) [°] |                          |                          |   |                          |                             |                              |  |
| Z1–B–Ni–Z2  | 118.56                   | 123.60                   | 126.87  | 121.21                   | 129.91                      | 125.60                       | 114.86   |

[a] Ref.<sup>[4]</sup> [b] Ref.<sup>[5]</sup> [c] Ref.<sup>[7a]</sup> [d] Space group  $C2/c$ .

(1-methyl-2-imidazolyl)methoxymethylborate,  $[\text{B}(\text{Im}^{N-\text{Me}})_2(\text{OMe})\text{Me}]^-$ , which is formed by the reaction of  $\text{Li}\cdot\text{L}^{\text{O}}\text{iPr}$  with  $\text{Ni}(\text{OAc})_2\cdot 4\text{H}_2\text{O}$  in  $\text{MeOH}$ .<sup>[5]</sup> The planar phenyl ring and the less sterically demanding oxygen atom of the methoxy group is located between two imidazolyl-attached *N*-methyl groups (see Figure 2). In these complexes, the boron-attached methyl groups are not directed towards the nickel center, and the dihedral angles of the two imidazolyl rings are larger than those found in  $\mathbf{1}^{\text{alkyl}}$  as summarized in Table 1.

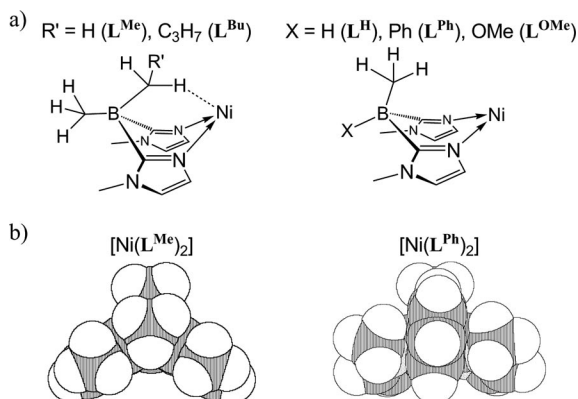


Figure 2. Comparison of the  $\text{L}^{\text{X}}\text{Ni}$  moieties. (a) Schematic diagram. (b) Space filling drawing of the half unit of  $\mathbf{1}^{\text{Me}}$  and  $\mathbf{1}^{\text{Ph}}$  viewing along B–Ni axis.

A structural isomer of the previously reported  $\mathbf{1}^{\text{Ph}}$  has also been characterized successfully. In this isomer,  $\mathbf{1}^{\text{Ph}'}$ , the phenyl substituent attached to the boron atom faces towards the nickel center and the geometry around the boron atom is similar to that found in  $\mathbf{1}^{\text{alkyl}}$ , i.e. the boron-attached methyl group is located between the two *N*-methyl groups with relatively small dihedral angles of the two imidazolyl rings. The phenyl-facing complex,  $\mathbf{1}^{\text{Ph}'}$ , was obtained by the reaction of  $\text{L}^{\text{Ph}}$  and  $[\text{Ni}^{\text{I}}\text{Cl}(\text{PPh}_3)_3]$ . Interconversion behavior between  $\mathbf{1}^{\text{Ph}}$  and  $\mathbf{1}^{\text{Ph}'}$  has not been observed, and the formation mechanism of  $\mathbf{1}^{\text{Ph}'}$  is unclear. However, the existence of the isomers  $\mathbf{1}^{\text{Ph}}$  and  $\mathbf{1}^{\text{Ph}'}$  suggests a flexible coordination behaviour of  $\text{L}^{\text{X}}$ , and that the rearrangement of the boron-attached groups on  $\text{L}^{\text{X}}$  is possible.

### Solution State Behavior of $\text{L}^{\text{alkyl}}$ in Homoleptic Complexes

In  $^1\text{H}$  NMR spectra recorded at  $-60^\circ\text{C}$ , the metal-directing  $\alpha\text{-CH}$  protons of Me or *n*Bu in  $\mathbf{1}^{\text{Me}}$  and  $\mathbf{1}^{\text{Bu}}$ , respectively, could be discriminated from that of the other boron-attached methyl group. The protons of one methyl group ( $\mathbf{1}^{\text{Me}}$ ) and the  $\alpha$ -methylene of *n*Bu ( $\mathbf{1}^{\text{Bu}}$ ) appear at  $\delta = 1.91$  and 3.07 ppm, respectively, whereas the remaining boron-attached methyl protons are observed at around 0.4 ppm (Figure 3). Notably, the  $\alpha\text{-CH}$  protons of the boron-attached alkyl groups in the free ligands were observed at  $\delta = 0.07$  ( $\text{L}^{\text{Me}}$ ) and 0.76 ( $\text{L}^{\text{Bu}}$ ) ppm. These observations clearly indicate that the molecular structures of  $\mathbf{1}^{\text{alkyl}}$  determined by X-ray crystallography are kept in the solution state. In

general, the metal-interacting “anagostic” protons are observed downfield, whereas the typical agostic protons show upfield shifts.<sup>[14,15]</sup> Similar downfield shifts of protons of the boron-attached alkyl groups have been observed in analogous nickel(II) complexes with dialkylbis(pyrazolyl)borates,  $[\text{Ni}^{\text{II}}(\{\text{B}(\text{pz})_2(\text{R}')_2\})_2]$  ( $\text{R}' = \text{Et}, \text{Bu}$ ).<sup>[10a,13b]</sup>

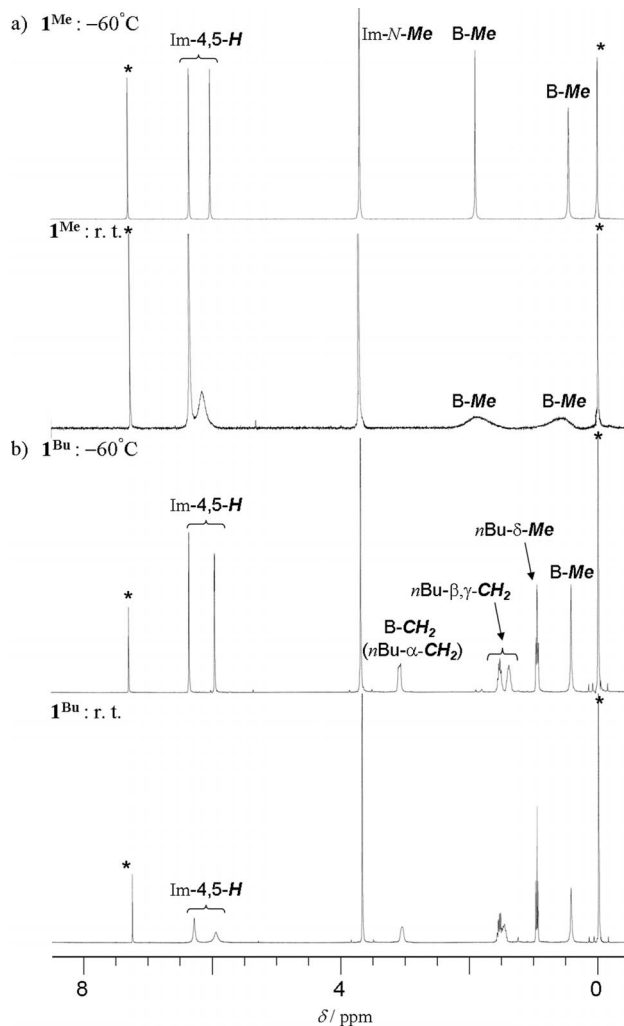
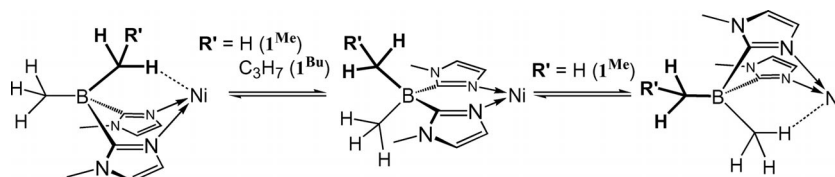


Figure 3. Variable temperature  $^1\text{H}$  NMR spectra of (a)  $\mathbf{1}^{\text{Me}}$  and (b)  $\mathbf{1}^{\text{Bu}}$ . Asterisks denote the signals attributed to impurities.

At ambient temperature,  $\mathbf{1}^{\text{alkyl}}$  shows fluxional behaviour indicated by broadening of the  $^1\text{H}$  NMR signals. Extreme broadening of all signals of  $\mathbf{1}^{\text{Me}}$  was observed, while the signal of the boron-attached methyl proton in  $\mathbf{1}^{\text{Bu}}$  was less broad. This difference reflects the degree of structural flexibility of  $\text{L}^{\text{alkyl}}$ . A plausible explanation in the case of  $\mathbf{1}^{\text{Me}}$  is that orientation exchange of the two methyl groups might occur with a butterfly-like flipping motion of the imidazolyl groups on  $\text{L}^{\text{Me}}$  as shown in Scheme 2. Another possible motion mechanism is that a ligand-dissociation process occurs as follows: (i) One of the two imidazolyl ligands dissociates, (ii) rotation occurs about the retained Ni–N bond, (iii) recoordination of the dissociated imidazolyl ligand occurs. In contrast, rearrangement of the boron-attached Me and *n*Bu

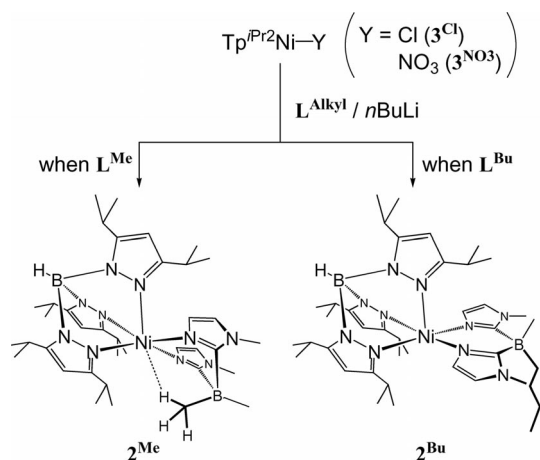
Scheme 2. Possible mechanism for the fluxional behaviour of  $L^{\text{alkyl}}$ .

groups on  $L^{\text{Bu}}$  would be difficult due to large steric hindrance between the *N*-Me groups and the  $\beta$ -methylene of *n*Bu if the boron-attached methyl group should face the nickel center in  $1^{\text{Bu}}$ .

### Synthesis and Characterization of Nickel(II) Complexes of $L^{\text{alkyl}}$ and $\text{Tp}^{i\text{Pr}2}$ [ $\text{Ni}^{\text{II}}(L^{\text{alkyl}})(\text{Tp}^{i\text{Pr}2})$ ]

As described above, the  $\alpha$ -CH of the alkyl substituents on  $L^{\text{alkyl}}$  lies in the vicinity of the metal center in the homoleptic complexes  $1^{\text{alkyl}}$ . In this case, no shield surrounding the nickel center exists. In order to clarify the controlling factor for the structure of the dialkylbis(imidazolyl)borate scaffold as well as the capability for C–H $\cdots$ M interactions in  $L^{\text{alkyl}}$ , we examined the effect of steric hindrance around the metal center, while retaining the interactive site of the  $\alpha$ -CH.

Reaction of the hindered  $\text{Tp}^{i\text{Pr}2}$  ligand complexes of nickel(II),  $[\text{Ni}^{\text{II}}(\text{X})(\text{Tp}^{i\text{Pr}2})]$  [ $\text{Tp}^{i\text{Pr}2}$  = hydrotris(3,5-diisopropyl-1-pyrazolyl)borate, X = Cl ( $3^{\text{Cl}}$ ) or  $\text{NO}_3$  ( $3^{\text{NO}_3}$ )],<sup>[16]</sup> with one equiv. of the lithium salt of  $L^{\text{alkyl}}$  (generated in situ by treatment of the protonated  $L^{\text{alkyl}}$  with *n*BuLi) at  $-80^\circ\text{C}$  yielded the desired mixed-ligand complex,  $[\text{Ni}^{\text{II}}(L^{\text{alkyl}})(\text{Tp}^{i\text{Pr}2})]$  ( $2^{\text{alkyl}}$ ; alkyl = Me or *n*Bu) (Scheme 3). Observation of the paramagnetically shifted  $^1\text{H}$  NMR signals of the blue-purple products suggested that the nickel(II) center ( $d^8$ ) adopts a high-spin electronic configuration. Notably, the homoleptic complexes,  $1^{\text{alkyl}}$ , were formed as by-products when the solution of the lithium salt of  $L^{\text{alkyl}}$  was added to the solution of  $\text{Tp}^{i\text{Pr}2}$  complex at room temperature. Therefore, the coordination ability of  $L^{\text{alkyl}}$  is higher than that of  $\text{Tp}^{i\text{Pr}2}$ .

Scheme 3. Synthesis of  $2^{\text{alkyl}}$ .

The molecular structures of  $2^{\text{alkyl}}$  were determined by X-ray crystallography (Figure 4 and Table 2). As expected from the high-spin state, the geometry of the nickel(II) centers in  $2^{\text{alkyl}}$  is square pyramidal supported by five nitrogen donors from the tridentate  $\text{Tp}^{i\text{Pr}2}$  and the bidentate  $L^{\text{alkyl}}$ . The values of a normalized measure of geometry of the five-coordinate center  $\tau$  ( $\tau = 0$  for a square pyramid,  $\tau = 1$  for a trigonal bipyramid with flat base) indicate that the geometry of the nickel center in  $2^{\text{Bu}}$  is slightly distorted ( $\tau = 0.050$ ), whereas that in  $2^{\text{Me}}$  is close to perfect square pyramidal ( $\tau = 0.003$ ). The average Ni– $N_L$  bond lengths are shorter than the Ni– $N_{\text{Tp}}$  distances in both  $2^{\text{alkyl}}$  complexes, which shows that the  $L^{\text{alkyl}}$  ligands are stronger donors compared to  $\text{Tp}^{i\text{Pr}2}$ . The nitrile moieties of the solvent molecules used for crystallization (EtCN for  $2^{\text{Me}}$  and MeCN for  $2^{\text{Bu}}$ ) did not coordinate to the nickel centers because the boron-attached alkyl groups covered the sixth coordination

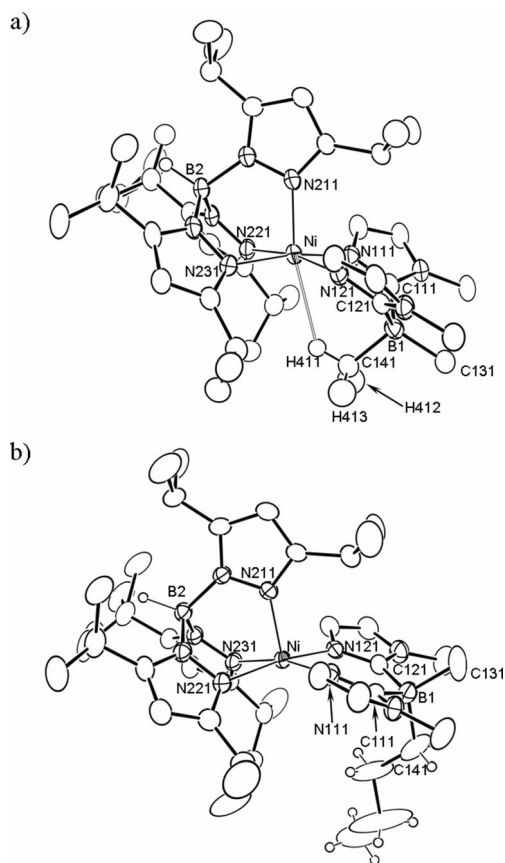
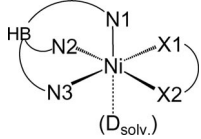
Figure 4. Molecular structures of (a)  $2^{\text{Me}}$  and (b)  $2^{\text{Bu}}$  drawn at 30% probability. Hydrogen atoms except those attached to boron in  $\text{Tp}^{i\text{Pr}2}$  and those of the alkyl groups in  $L^{\text{alkyl}}$  are omitted for clarity.

Table 2. Structural parameters for the mixed-ligand complexes **2<sup>alkyl</sup>** and **3<sup>NO<sub>3</sub>(NCMe)</sup>**.


| Complex  | <b>2<sup>Me</sup></b>       | <b>2<sup>Bu</sup></b>       | <b>3<sup>NO<sub>3</sub>(NCMe)</sup></b> |
|--|-----------------------------|-----------------------------|---|
| Equatorial donor   | N ( <b>L<sup>Me</sup></b> ) | N ( <b>L<sup>Bu</sup></b> ) | O ( $\kappa^2$ -NO <sub>3</sub> )       |
| Coordination number of Ni  | 5                           | 5                           | 6                                       |
| $\tau$ value <sup>[a]</sup>  | 0.003                       | 0.050                       | 0.004 <sup>[b]</sup>                    |
| Bond lengths [Å]   |                             |                             |   |
| Ni–X1  | 2.004(4)                    | 2.013(3)                    | 2.1311(18)                              |
| Ni–X2  | 2.022(3)                    | 2.018(3)                    | 2.122(2)                                |
| Average of Ni–X  | 2.013                       | 2.016                       | 2.128                                   |
| Ni–N1  | 2.051(3)                    | 2.014(3)                    | 2.1085(18)                              |
| Ni–N2  | 2.094(3)                    | 2.115(3)                    | 2.038(2)                                |
| Ni–N3  | 2.065(3)                    | 2.099(3)                    | 2.0316(19)                              |
| Average of Ni–N <sub>TP</sub>  | 2.070                       | 2.076                       | 2.059                                   |
| Ni–D <sub>solv</sub>   | –                           | –                           | 2.196(2)                                |
| B1–C111  | 1.627(6)                    | 1.617(6)                    | –                                       |
| B1–C121  | 1.628(6)                    | 1.616(6)                    | –                                       |
| B1–C131  | 1.633(6)                    | 1.657(7)                    | –                                       |
| B1–C141  | 1.644(6)                    | 1.661(7)                    | –                                       |
| Ni $\cdots$ H <sub>alkyl</sub>   | 2.66(4)                     | 3.712                       | –                                       |
| Distance from the plane N111–C111–C121–N121 (= N <sub>2</sub> C <sub>2</sub> ) [Å]         |                             |                             |   |
| N <sub>2</sub> C <sub>2</sub> $\cdots$ Ni  | 0.601(5)                    | 0.465(5)                    | –                                       |
| N <sub>2</sub> C <sub>2</sub> $\cdots$ B1  | 0.662(6)                    | 0.080(7)                    | –                                       |
| Bond angles [°]  |                             |                             |   |
| X1–Ni–X2   | 89.51(14)                   | 89.93(11)                   | 60.36(8)                                |
| X1–Ni–N1   | 98.00(14)                   | 99.56(12)                   | 96.45(8)                                |
| X1–Ni–N2   | 92.31(14)                   | 93.08(11)                   | 103.17(8)                               |
| X1–Ni–N3   | 169.26(14)                  | 166.39(13)                  | 162.90(8)                               |
| X2–Ni–N1   | 97.82(14)                   | 98.05(13)                   | 96.68(7)                                |
| X2–Ni–N2   | 169.10(13)                  | 169.37(13)                  | 163.16(8)                               |
| X2–Ni–N3   | 92.79(14)                   | 92.59(11)                   | 102.77(8)                               |
| N1–Ni–N2   | 92.57(13)                   | 91.51(12)                   | 88.32(8)                                |
| N1–Ni–N3   | 92.08(13)                   | 93.33(12)                   | 87.91(8)                                |
| N2–Ni–N3   | 83.52(13)                   | 82.16(11)                   | 93.45(8)                                |
| C111–B1–C121   | 105.4(3)                    | 109.4(3)                    | [X1–Ni–D <sub>solv</sub> ; 83.07(9)]    |
| C111–B1–C131   | 115.9(4)                    | 105.9(4)                    | [X2–Ni–D <sub>solv</sub> ; 82.93(8)]    |
| C111–B1–C141   | 107.3(4)                    | 109.6(4)                    | [N1–Ni–D <sub>solv</sub> ; 179.49(9)]   |
| C121–B1–C131   | 115.0(4)                    | 108.8(4)                    | [N2–Ni–D <sub>solv</sub> ; 91.96(8)]    |
| C121–B1–C141   | 105.6(4)                    | 108.4(4)                    | [N3–Ni–D <sub>solv</sub> ; 92.50(9)]    |
| C131–B1–C141   | 107.0(4)                    | 114.7(4)                    |   |
| Torsion angles of Z1–B–Ni–Z2<br>(Z1 and Z2 denote the centers of the imidazolyl rings) [°] |                             |                             |   |
| Z1–Ni–B1–Z2  | 129.87                      | 160.30                      | –                                       |

[a]  $\tau = (\beta - \alpha)/60$ , where  $\alpha$  and  $\beta$  denote values of the first and second largest angles around five-coordinate metal center, respectively. [b] Upon the calculation of this value, D<sub>solv</sub> is omitted.

site (Figure S2). In contrast, the nickel(II) nitrato complex **3<sup>NO<sub>3</sub></sup>**, the starting material of **2<sup>Bu</sup>**, has an MeCN ligand to form [Ni<sup>II</sup>( $\kappa^2$ -O, O'-NO<sub>3</sub>)(Tp<sup>iPr2</sup>)(NCMe)] [**3<sup>NO<sub>3</sub>(NCMe)</sup>**; Figure S1].<sup>[17]</sup>

Sterically induced C–H $\cdots$ M interactions are observed in the **L<sup>Me</sup>** complex **2<sup>Me</sup>** as well as the corresponding homoleptic complex **1<sup>Me</sup>**. The C–H $\cdots$ Ni distance in **2<sup>Me</sup>** is somewhat longer than that in **1<sup>Me</sup>** and similar to that found for complexes of [B(pz)<sub>2</sub>(BBN)]<sup>–</sup>, [Co<sup>II</sup>[B(pz)<sub>2</sub>(BBN)](Tp<sup>iPr,4-Br</sup>)] (H $\cdots$ Co; 2.61 Å) and [Co<sup>II</sup>[(B(pz)<sub>2</sub>(BBN))<sub>2</sub>]] (H $\cdots$ Co; 2.166 Å).<sup>[13]</sup> In contrast, no interaction between the  $\alpha$ -CH of the *n*-butyl group and the nickel center exists in **2<sup>Bu</sup>** due to steric repulsion between the nickel-surrounding *i*Pr groups of Tp<sup>iPr2</sup> and the *sp*<sup>3</sup>-hydrocarbon chain of the *n*Bu group on **L<sup>Bu</sup>**. The arrangement of the two imidazole groups comes close to coplanar, indicated by the largest dihedral angle between the two rings (see Table 1 and Table 2). Moreover, the boron-attached carbon atoms of the Me and *n*Bu groups are located away from the nickel center. Similar structural characteristics around the boron center are found in complexes with the acetoxy group-incorporated ligand [B(Im<sup>N-Me</sup>)<sub>2</sub>(OAc)Me]<sup>–</sup> (= **L<sup>OAc</sup>**).<sup>[5]</sup> These differences clearly demonstrate that the structural environment around the metal center also influences the arrangement of the imidazolyl groups on **L<sup>alkyl</sup>** as well as the alkyl groups. The sterically enforced C–H $\cdots$ M interaction formed in our complexes of nickel(II) is weak and comparable to the crystal packing force.

## Conclusions

The coordination properties of alkylmethylbis(imidazolyl)borate ligands, **L<sup>alkyl</sup>**, have been investigated. In its homoleptic complexes, **1<sup>alkyl</sup>**, one of the two alkyl groups attached to the boron center faces the nickel(II) center due to the steric repulsion between the *N*-methyl groups of the imidazolyl ligands and the other boron-attached methyl group. The resulting configuration of the boron-attached alkyl groups leads to anagostic C–H $\cdots$ Ni interactions. The molecular structures of **1<sup>alkyl</sup>** are essentially retained in the solution state, although **L<sup>alkyl</sup>** exhibits fluxional behavior. In the mixed ligand complexes, **2<sup>alkyl</sup>**, steric hindrance around the metal center also affects the orientation of the boron-attached alkyl and imidazolyl groups of **L<sup>alkyl</sup>**.

In summary, the structure of the dialkylbis(imidazolyl)borate scaffold is somewhat flexible and the steric hindrance around both the boron and metal centers is a dominant factor for the conformation of the boron-attached functional groups.

## Experimental Section

**Instrumentation:** IR measurements were carried out from KBr pellets with JASCO FT/IR-5300 and FT/IR-550 spectrometers. NMR spectra were recorded at room temperature with JEOL GX-270 (<sup>1</sup>H; 270 MHz) and EX-400 (<sup>1</sup>H; 400 MHz and <sup>13</sup>C; 100 MHz) spectrometers. Chemical shifts are reported in ppm downfield from internal SiMe<sub>4</sub>. Field desorption (FD) mass spectra were recorded with a JEOL JMS-700 mass spectrometer.

**Materials and Methods:** All solvents used were purified by literature methods: Et<sub>2</sub>O and pentane (Na–K alloy), toluene (Na), CH<sub>2</sub>Cl<sub>2</sub>,

CHCl<sub>3</sub> and MeCN (P<sub>2</sub>O<sub>5</sub>), MeOH [Mg(OMe)<sub>2</sub>] were treated with appropriate drying agents, distilled, and stored under argon.<sup>[18]</sup> Commercially available reagents were of the highest grade and were used without further purification. All manipulations for the preparation of catalysts were performed under argon by using glove box or standard Schlenk techniques. Starting materials for the organoborate ligands **L<sup>R</sup>** (R = Me, Bu, H), namely the chlorinated borate compound [B(Im<sup>N-Me</sup>)<sub>2</sub>(Cl)Me]<sup>-</sup> (**L<sup>Cl</sup>**)<sup>[4]</sup> and its precursor [B(Im<sup>N-Me</sup>)<sub>2</sub>(O*i*Pr)Me]<sup>-</sup> (**L<sup>O*i*Pr</sup>**)<sup>[4]</sup> bis(1-methyl-2-imidazolyl)methylphenylborate [B(Im<sup>N-Me</sup>)<sub>2</sub>(Ph)Me]<sup>-</sup> (**L<sup>Ph</sup>**)<sup>[4]</sup> [Ni<sup>I</sup>Cl(PPh<sub>3</sub>)<sub>3</sub>]<sup>[19]</sup> and [Ni<sup>II</sup>(Cl)(Tp<sup>Pr2</sup>)] (**3<sup>Cl</sup>**)<sup>[16]</sup> were prepared according to previously reported procedures.

### Synthesis of the Compounds

**H[B(Im<sup>N-Me</sup>)<sub>2</sub>Me<sub>2</sub>] (H·L<sup>Me</sup>):** The chlorinated borate **L<sup>Cl</sup>**, generated in situ from the reaction of Li·L<sup>O*i*Pr</sup> (4.05 mmol) with anhydrous HCl (Et<sub>2</sub>O solution), was suspended in a Et<sub>2</sub>O/toluene mixture and chilled to -78 °C. An Et<sub>2</sub>O solution of methylolithium (1.6 M; 10 mL) was added slowly. The mixture was gradually warmed to ambient temperature, with continuous stirring for 10 h. The reaction mixture was heated for 8 h, and the volatile solvents were removed under vacuum. The product was washed with H<sub>2</sub>O and pentane, and then dried under vacuum. This spectroscopically pure **H·L<sup>Me</sup>** was obtained as a white powder (518 mg; 2.54 mmol; 63% yield). C<sub>10</sub>H<sub>17</sub>BN<sub>4</sub> (204.08; **H·L<sup>Me</sup>**): calcd. C 58.85, H 8.40, N 27.45; found C 58.52, H 8.51, N 27.08. IR (KBr):  $\tilde{\nu}$  = 3513 (vs,  $\nu_{\text{NH}}$ ), 3177 (s), 2927 (s,  $\nu_{\text{CH}}$ ), 2829 (s,  $\nu_{\text{CH}}$ ), 2050 (w), 1582 (vs), 1470 (vs), 1444 (vs), 1355 (vs), 1309 (m), 1293 (s,  $\nu_{\text{BC}}$ ), 1273 (s), 1249 (s), 1164 (m), 1110 (vs), 1033 (m), 1003 (vs), 984 (m), 932 (w), 916 (w), 865 (m), 843 (w), 800 (w), 755 (s), 738 (vs), 714 (vs), 695 (s), 682 (m), 613 (w), 496 (m), 463 (m), 427 (w), 409 (w). <sup>1</sup>H NMR (CDCl<sub>3</sub>):  $\delta$  = 0.07 (br., 6 H, *Me-B*), 3.78 (s, 6 H, *Me-N*), 6.79 (d,  $J$  = 1.5 Hz, 2 H, *5-H<sub>im</sub>*), 6.95 (d,  $J$  = 1.5 Hz, 2 H, *4-H<sub>im</sub>*), 13.34 (br., 1 H, *H-N*) ppm. <sup>13</sup>C{<sup>1</sup>H} NMR (CDCl<sub>3</sub>):  $\delta$  = 6.7 (br., *Me-B*), 35.0 (q,  $J_{\text{CH}}$  = 139.1 Hz, *Me-N*), 119.4 (dd,  $J_{\text{CH}}$  = 190.0,  $2J_{\text{CH}}$  = 10.4 Hz, *4-C<sub>im</sub>*), 121.1 (ddq,  $J_{\text{CH}}$  = 188.9,  $2J_{\text{CH}}$  = 13.5,  $3J_{\text{CH}}$  = 3.1 Hz, *5-C<sub>im</sub>*), 171.3 (br., *2-C<sub>im</sub>*) ppm.

**H[B(Im<sup>N-Me</sup>)<sub>2</sub>(*n*Bu)Me] (H·L<sup>Bu</sup>):** **H·L<sup>Bu</sup>** was prepared according to the procedure for **H·L<sup>Me</sup>**. Instead of MeLi, a hexane solution of *n*-butyllithium (1.5 M; 8 mL) was added to **L<sup>Cl</sup>** (3.58 mmol). Spectroscopically pure **H·L<sup>Bu</sup>** was obtained as a white powder (670 mg; 2.72 mmol; 76% yield). C<sub>13</sub>H<sub>23</sub>BN<sub>4</sub> (246.16; **H·L<sup>Bu</sup>**): calcd. C 63.43, H 9.42, N 22.76; found C 63.77, H 9.05, N 22.40. IR (KBr):  $\tilde{\nu}$  = 3413 (vs,  $\nu_{\text{NH}}$ ), 3140 (s), 3102 (s,  $\nu_{\text{CH}}$ ), 2909 (vs,  $\nu_{\text{H}}$ ), 2687 (s), 2007 (m), 1585 (s), 1483 (s), 1444 (s), 1409 (s), 1357 (s), 1292 (s,  $\nu_{\text{BC}}$ ), 1278 (vs), 1203 (w), 1157 (m), 1115 (vs), 1090 (w), 1053 (m), 1021 (m), 988 (m), 954 (m), 925 (m), 881 (m), 841 (w), 734 (vs), 685 (m), 644 (w), 532 (w), 471 (w), 420 (w), 404 (w). <sup>1</sup>H NMR (CDCl<sub>3</sub>):  $\delta$  = 0.05 (br., 3 H, *Me-B*), 0.56 (vdq,  $J$  = 6.62, 2.58 Hz, 2 H, CH<sub>3</sub>CH<sub>2</sub>CH<sub>2</sub>CH<sub>2</sub>-B), 0.70 (t,  $J$  = 7.26 Hz, 3 H, CH<sub>3</sub>CH<sub>2</sub>CH<sub>2</sub>CH<sub>2</sub>-B),  $\approx$  0.76 (br., 2 H, CH<sub>3</sub>CH<sub>2</sub>CH<sub>2</sub>CH<sub>2</sub>-B), 1.07 (dt, 2 H, CH<sub>3</sub>CH<sub>2</sub>CH<sub>2</sub>CH<sub>2</sub>-B), 3.78 (s, 6 H, *Me-N*), 6.78 (d,  $J$  = 1.46 Hz, 2 H, *5-H<sub>im</sub>*), 6.95 (d,  $J$  = 1.46 Hz, 2 H, *4-H<sub>im</sub>*), 14.5 (br., 1 H, *H-N*) ppm. <sup>13</sup>C{<sup>1</sup>H} NMR (CDCl<sub>3</sub>):  $\delta$  = 6.0 (br., *Me-B*), 14.1 [qt,  $J_{\text{CH}}$  = 119.5,  $2J_{\text{CH}}$  = 3.7 Hz, CH<sub>3</sub>(CH<sub>2</sub>)<sub>3</sub>-B], 24.0 (br., C<sub>3</sub>H<sub>7</sub>CH<sub>2</sub>-B), 26.3 [t,  $J_{\text{CH}}$  = 125.0 Hz, CH<sub>3</sub>(CH<sub>2</sub>)<sub>2</sub>CH<sub>2</sub>-B], 31.1 [t,  $J_{\text{CH}}$  = 117.7 Hz, CH<sub>3</sub>(CH<sub>2</sub>)<sub>2</sub>CH<sub>2</sub>-B], 34.9 (q,  $J_{\text{CH}}$  = 139.7 Hz, *Me-N*), 119.3 (dd,  $J_{\text{CH}}$  = 189.4,  $2J_{\text{CH}}$  = 11.0 Hz, *4-C<sub>im</sub>*), 121.0 (ddq,  $J_{\text{CH}}$  = 189.4,  $2J_{\text{CH}}$  = 14.7,  $3J_{\text{CH}}$  = 3.7 Hz, *5-C<sub>im</sub>*), 171.0 (br., *2-C<sub>im</sub>*) ppm.

**H[B(Im<sup>N-Me</sup>)<sub>2</sub>(H)Me] (H·L<sup>H</sup>):** **H·L<sup>H</sup>** was prepared according to the procedure for **H·L<sup>Me</sup>**. Instead of MeLi, a pentane solution of *tert*-butyllithium (1.54 M; 8 mL) was added to **L<sup>Cl</sup>** (3.86 mmol). Solid

white **H·L<sup>H</sup>** was obtained in 22% yield (159 mg, 0.84 mmol). C<sub>9</sub>H<sub>15</sub>BN<sub>4</sub> (190.05; **H·L<sup>H</sup>**): calcd. C 56.88, H 7.96, N 29.48; found C 57.02, H 7.78, N 29.15. IR (KBr):  $\tilde{\nu}$  = 3133 (s), 2926 (vs,  $\nu_{\text{CH}}$ ), 2288 (m,  $\nu_{\text{BH}}$ ), 1568 (s), 1467 (s), 1448 (s), 1412 (m), 1362 (m), 1279 (s,  $\nu_{\text{BC}}$ ), 1259 (s), 1192 (m), 1092 (s), 1025 (s), 934 (s), 803 (m), 731 (s), 646 (w), 584 (w), 503 (w), 432 (w), 415 (w). <sup>1</sup>H NMR (CDCl<sub>3</sub>):  $\delta$  = -0.09 (br., 3 H, *Me-B*), 3.75 (s, 6 H, *Me-N*), 6.83 (d,  $J$  = 1.57 Hz, 2 H, *5-H<sub>im</sub>*), 7.00 (d,  $J$  = 1.57 Hz, 2 H, *4-H<sub>im</sub>*), 14.8 (br., 1 H, *H-N*) ppm. <sup>13</sup>C{<sup>1</sup>H} NMR (CDCl<sub>3</sub>):  $\delta$  = 3.5 (br., *Me-B*), 32.9 (q,  $J_{\text{CH}}$  = 139.1 Hz, *Me-N*), 120.1 (dd,  $J_{\text{CH}}$  = 191.0,  $2J_{\text{CH}}$  = 11.4 Hz, *4-C<sub>im</sub>*), 120.3 (br., *5-C<sub>im</sub>*), 154.0 (br., *2-C<sub>im</sub>*) ppm.

**[Ni(L<sup>Me</sup>)<sub>2</sub>] (1<sup>Me</sup>):** A CH<sub>2</sub>Cl<sub>2</sub> solution (20 mL) of **H·L<sup>Me</sup>** (133 mg; 0.65 mmol) was added slowly to a methanol solution (15 mL) of Ni(OAc)<sub>2</sub>·4H<sub>2</sub>O (81 mg; 0.33 mmol). The reaction mixture was stirred for 1 h before the solvents were removed under vacuum. The product was extracted into CH<sub>2</sub>Cl<sub>2</sub> (30 mL) to remove any inorganic impurities. After the CH<sub>2</sub>Cl<sub>2</sub> was removed, yellow crystals of **1<sup>Me</sup>**, suitable for X-ray diffraction analysis, were obtained by recrystallization from CH<sub>3</sub>CN/CH<sub>2</sub>Cl<sub>2</sub> (68 mg; 0.15 mmol; 45% yield). C<sub>20</sub>H<sub>32</sub>B<sub>2</sub>N<sub>8</sub>Ni (464.84; **1<sup>Me</sup>**): calcd. C 51.68, H 6.94, N 24.11; found C 51.22, H 6.92, N 24.13. IR (KBr):  $\tilde{\nu}$  = 3145 (m,  $\nu_{\text{CH}}$ ), 3126 (s,  $\nu_{\text{CH}}$ ), 3117 (s,  $\nu_{\text{CH}}$ ), 2921 (vs,  $\nu_{\text{CH}}$ ), 2899 (vs,  $\nu_{\text{CH}}$ ), 2836 (s,  $\nu_{\text{CH}}$ ), 2808 (s,  $\nu_{\text{CH}}$ ), 1668 (w), 1550 (m), 1453 (vs), 1407 (vs), 1387 (s), 1291 (vs,  $\nu_{\text{BC}}$ ), 1265 (s), 1165 (vs), 1154 (vs), 1084 (m), 1062 (m), 1043 (s), 1024 (s), 987 (s), 960 (s), 844 (w), 835 (w), 829 (w) 816 (w), 745 (s), 731 (vs), 721 (vs), 708 (vs), 696 (vs), 613 (m), 511 (m), 476 (m), 409 (m). <sup>1</sup>H NMR (CDCl<sub>3</sub>):  $\delta$  = 0.52 (br., 3 H, *Me-B*), 1.83 (br., 3 H, *Me-B*), 3.68 (s, 6 H, *Me-N*), 6.13 (br., 2 H, *5-H<sub>im</sub>*), 6.32 (br., 2 H, *4-H<sub>im</sub>*) ppm.

**[Ni(L<sup>Bu</sup>)<sub>2</sub>] (1<sup>Bu</sup>):** A CH<sub>2</sub>Cl<sub>2</sub> solution (20 mL) of **H·L<sup>Bu</sup>** (289 mg; 1.18 mmol) was added dropwise to a methanol solution (15 mL) of Ni(OAc)<sub>2</sub>·4H<sub>2</sub>O (146 mg; 0.59 mmol). The reaction mixture was stirred overnight, and then the solvents were removed under vacuum. The product was extracted into CH<sub>2</sub>Cl<sub>2</sub> (20 mL) to remove any inorganic impurities. After the removal of CH<sub>2</sub>Cl<sub>2</sub>, crystallization from CH<sub>2</sub>Cl<sub>2</sub>/hexane afforded yellow crystals of **1<sup>Bu</sup>** (82 mg; 0.15 mmol; 25% yield). C<sub>26</sub>H<sub>44</sub>B<sub>2</sub>N<sub>8</sub>Ni (549.00; **1<sup>Bu</sup>**): calcd. C 56.88, H 8.08, N 20.41; found C 56.55, H 8.22, N 20.29. IR (KBr):  $\tilde{\nu}$  = 3149 (m,  $\nu_{\text{CH}}$ ), 3121 (s,  $\nu_{\text{CH}}$ ), 2946 (vs,  $\nu_{\text{CH}}$ ), 2925 (vs,  $\nu_{\text{CH}}$ ), 2877 (vs,  $\nu_{\text{CH}}$ ), 2863 (vs,  $\nu_{\text{CH}}$ ), 2835 (vs,  $\nu_{\text{CH}}$ ), 2785 (s,  $\nu_{\text{CH}}$ ), 1657 (w), 1546 (m), 1452 (vs), 1411 (s), 1388 (m), 1368 (w), 1287 (vs,  $\nu_{\text{BC}}$ ), 1203 (m), 1166 (s), 1153 (s), 1085 (m), 1062 (s), 1012 (m), 990 (s), 955 (m), 932 (m), 879 (w), 862 (w) 846 (w), 830 (w), 792 (w), 741 (m), 733 (s), 717 (vs), 699 (s), 643 (w), 626 (w), 512 (w), 425 (m), 413 (w), 407 (w). <sup>1</sup>H NMR (CDCl<sub>3</sub>):  $\delta$  = 0.43 (s, 3 H, *Me-B*), 0.96, ( $J$  = 7.28 Hz, 3 H, CH<sub>3</sub>CH<sub>2</sub>CH<sub>2</sub>CH<sub>2</sub>-B), 1.45–1.58 (br., 4 H, CH<sub>3</sub>CH<sub>2</sub>CH<sub>2</sub>CH<sub>2</sub>-B), 3.06 (br., 2 H, CH<sub>3</sub>CH<sub>2</sub>CH<sub>2</sub>CH<sub>2</sub>-B), 3.68 (s, 6 H, *Me-N*), 5.96 (br., 2 H, *5-H<sub>im</sub>*), 6.29 (br., 2 H, *4-H<sub>im</sub>*) ppm.

**[Ni(L<sup>H</sup>)<sub>2</sub>] (1<sup>H</sup>):** A CH<sub>2</sub>Cl<sub>2</sub> solution (20 mL) of **H·L<sup>H</sup>** (54 mg; 0.28 mmol) was added dropwise to a methanol solution (10 mL) of Ni(OAc)<sub>2</sub>·4H<sub>2</sub>O (36 mg; 0.14 mmol). The reaction mixture was stirred for 1 h, the solvents were removed under vacuum, and the product was extracted into toluene (20 mL). After removal of the solvent, crystallization from CH<sub>2</sub>Cl<sub>2</sub>/MeCN afforded yellow crystals of **1<sup>H</sup>** (50 mg; 0.11 mmol; 81% yield). C<sub>18.5</sub>H<sub>29</sub>B<sub>2</sub>ClN<sub>8</sub>Ni (479.25; **1<sup>H</sup>**·0.5CH<sub>2</sub>Cl<sub>2</sub>): calcd. C 46.36, H 6.10, N 23.38; found C 46.86, H 6.44, N 23.90. IR (KBr):  $\tilde{\nu}$  = 3153 (m,  $\nu_{\text{CH}}$ ), 3130 (s,  $\nu_{\text{CH}}$ ), 2927 (vs,  $\nu_{\text{CH}}$ ), 2910 (vs,  $\nu_{\text{CH}}$ ), 2818 (s,  $\nu_{\text{CH}}$ ), 2316 (vs,  $\nu_{\text{BH}}$ ), 2251 (m), 2120 (m), 1685 (w), 1643 (w), 1545 (m), 1456 (vs), 1398 (s), 1321 (w), 1290 (s,  $\nu_{\text{BC}}$ ), 1264 (s), 1200 (m), 1156 (vs), 1147 (vs), 1095 (s), 1065 (vs), 1018 (s), 971 (m), 928 (m), 842 (m), 833 (m), 822 (m) 801 (m), 745 (s), 731 (vs), 720 (vs), 703 (vs), 624 (w), 469

(m), 419 (w).  $^1\text{H}$  NMR ( $\text{CDCl}_3$ ):  $\delta = 1.00$  (br., 3 H, *Me-B*), 3.68 (s, 6 H, *Me-N*), 5.91 (br., 2 H, *5-H<sub>im</sub>*), 6.44 (br., 2 H, *4-H<sub>im</sub>*) ppm.

**[Ni(L<sup>Ph</sup>)<sub>2</sub> (1<sup>Ph</sup>):** A toluene solution (25 mL) of **H·L<sup>Ph</sup>** (171 mg; 0.64 mmol) was added dropwise to a methanol solution (20 mL) of **[NiCl(PPh<sub>3</sub>)<sub>3</sub>]** (572 mg; 0.65 mmol). After the reaction mixture was stirred overnight, the mixture was allowed to settle for 1 h before removal of the resultant supernatant by decantation. The residue was dried under vacuum. Crystallization from  $\text{CH}_3\text{CN}/\text{THF}$  afforded pale yellow crystals of **1<sup>Ph</sup>** (60 mg; 0.10 mmol; 32% yield).  $\text{C}_{34}\text{H}_{44}\text{B}_2\text{N}_8\text{NiO}$  (661.08; **1<sup>Ph</sup>·THF**): calcd. C 61.77, H 6.71, N 16.95; found C 61.55, H 6.50, N 16.93. IR (KBr):  $\tilde{\nu} = 3160$  (m,  $\nu_{\text{CH}}$ ), 3129 (vs,  $\nu_{\text{CH}}$ ), 3055 (s,  $\nu_{\text{CH}}$ ), 2992 (vs,  $\nu_{\text{CH}}$ ), 2928 (vs,  $\nu_{\text{CH}}$ ), 2850 (vs,  $\nu_{\text{CH}}$ ), 2697 (w), 1938 (w), 1860 (w), 1806 (w), 1673 (w), 1648 (w), 1578 (m), 1542 (m), 1481 (s), 1454 (vs), 1404 (s), 1292 (vs), 1286 (vs,  $\nu_{\text{BC}}$ ), 1154 (vs), 1069 (s), 1032 (m), 1011 (m), 991 (s), 938 (vs), 901 (s), 837 (w), 777 (s).  $^1\text{H}$  NMR ( $\text{CDCl}_3$ ):  $\delta = 1.10$  (br., 3 H, *Me-B*), 4.50 (s, 6 H, *Me-N*), 5.7–7.5 (br., 9 H, *4-* and *5-H<sub>im</sub>* and Ph) ppm.

**[Ni(L<sup>Me</sup>)(Tp<sup>Pr2</sup>) (2<sup>Me</sup>):** A 1.6 mL *n*-hexane solution of *n*-butyllithium (0.19 mL; 0.30 mmol) was slowly added to a THF solution (10 mL) of **H·L<sup>Me</sup>** (62 mg, 0.30 mmol) at  $-80^\circ\text{C}$ . The resulting mixture was warmed gradually to ambient temperature and stirred for 30 min. This **Li·L<sup>Me</sup>** solution was added dropwise to a THF solution (10 mL) of **[Ni<sup>II</sup>(Cl)(Tp<sup>Pr2</sup>)]** (172 mg, 0.30 mmol) at  $-80^\circ\text{C}$ . The reaction mixture was warmed gradually to ambient temperature and stirred for 2 h. The product was extracted into pentane to remove LiCl. Evaporation of the pentane solution followed by recrystallization from EtCN at  $-30^\circ\text{C}$  afforded blue-purple crystalline **2<sup>Me</sup>** (140 mg; 0.19 mmol; 63% yield).  $\text{C}_{37}\text{H}_{62}\text{B}_2\text{N}_{10}\text{Ni}$  (727.27; **2<sup>Me</sup>**): calcd. C 61.11, H 8.59, N 19.26; found C 60.62, H 8.57, N 19.15. IR (KBr):  $\tilde{\nu} = 3122$  (w,  $\nu_{\text{CH}}$ ), 2966 (vs,  $\nu_{\text{CH}}$ ), 2927 (vs,  $\nu_{\text{CH}}$ ), 2867 (vs,  $\nu_{\text{CH}}$ ), 2835 (m,  $\nu_{\text{CH}}$ ), 2806 (w), 2536 (m,  $\nu_{\text{BH}}$ ), 1684 (w), 1537 (s), 1471 (s), 1429 (m), 1395 (s), 1380 (s), 1362 (s), 1303 (s,  $\nu_{\text{BC}}$ ), 1284 (s,  $\nu_{\text{BC}}$ ), 1175 (s), 1143 (m), 1128 (m), 1105 (w), 1051 (s), 1017 (m), 997 (m), 969 (s), 944 (w), 922 (w), 900 (w), 878 (w), 838 (w), 823 (m), 787 (s), 765 (m), 738 (w), 714 (s), 692 (m), 660 (m).  $^1\text{H}$  NMR ( $\text{C}_6\text{D}_6$ ):  $\delta = -0.2, 2.4, 6.8, 7.6, 45.6, 61.1$  ppm. FD-MS:  $m/z = 727$  [ $\text{M}^+$ ], 712 [ $\text{M} - \text{Me}$ ] $^+$ .

**[Ni(L<sup>Bu</sup>)(Tp<sup>Pr2</sup>) (2<sup>Bu</sup>):** A 1.6 mL *n*-hexane solution of *n*-butyllithium (0.44 mL; 0.70 mmol) was slowly added to a THF solution (10 mL) of **H·L<sup>Bu</sup>** (172 mg; 0.70 mmol) at  $-80^\circ\text{C}$ . The resulting mixture was warmed gradually to ambient temperature and stirred for 30 min. This **Li·L<sup>Me</sup>** solution was added dropwise to a THF solution (10 mL) of **[Ni<sup>II</sup>(NO<sub>3</sub>)(Tp<sup>Pr2</sup>)]** (410 mg; 0.70 mmol) at  $-80^\circ\text{C}$ . The reaction mixture was warmed gradually to ambient temperature and stirred for 2 h. The product was extracted into pentane. Evaporation of the pentane solution followed by recrystallization from MeCN at  $-30^\circ\text{C}$  afforded blue-purple crystalline **2<sup>Bu</sup>** (323 mg; 0.42 mmol; 60% yield).  $\text{C}_{40}\text{H}_{68}\text{B}_2\text{N}_{10}\text{Ni}$  (769.35; **2<sup>Bu</sup>**): calcd. C 62.45, H 8.91, N 18.21; found C 62.58, H 8.76, N 18.23. IR (KBr):  $\tilde{\nu} = 3123$  (w,  $\nu_{\text{CH}}$ ), 2965 (vs,  $\nu_{\text{CH}}$ ), 2928 (vs,  $\nu_{\text{CH}}$ ), 2870 (vs,  $\nu_{\text{CH}}$ ), 2835 (m,  $\nu_{\text{CH}}$ ), 2781 (w), 2540 (m,  $\nu_{\text{BH}}$ ), 1539 (s), 1459 (s), 1429 (m), 1395 (s), 1380 (s), 1362 (s), 1302 (s,  $\nu_{\text{BC}}$ ), 1282 (s,  $\nu_{\text{BC}}$ ), 1175 (s), 1143 (m), 1128 (m), 1105 (w), 1053 (s), 992 (m), 953 (m), 941 (m), 902 (w), 879 (w), 842 (w), 823 (m), 791 (s), 762 (m), 717 (s), 694 (m), 661 (m).  $^1\text{H}$  NMR ( $\text{C}_6\text{D}_6$ ):  $\delta = -10.9, -0.6, 2.7, 6.9, 7.6, 42.5, 61.2$  ppm. FD-MS:  $m/z = 769$  [ $\text{M}^+$ ], 712 [ $\text{M} - n\text{Bu}$ ] $^+$ .

**X-ray Data Collection and Structural Determinations:** Diffraction measurements of **1<sup>Me</sup>** and **3<sup>NO3</sup>(NCMe)·2MeCN** were performed with a Rigaku AFC-7R automated four-circle diffractometer. A molybdenum X-ray source equipped with a graphite monochromator (Mo- $K_\alpha$ ,  $\lambda = 0.71069 \text{ \AA}$ ) was used. Data collection was carried out at room temperature ( $23^\circ\text{C}$ ). Diffraction measurements of **1<sup>Bu</sup>**, **1<sup>H</sup>·CH<sub>2</sub>Cl<sub>2</sub>**, **1<sup>Ph</sup>·THF**, **2<sup>Me</sup>·2EtCN** and **2<sup>Bu</sup>** were made on a Rigaku RAXIS IV imaging plate area detector with Mo- $K_\alpha$  radiation ( $\lambda = 0.71069 \text{ \AA}$ ). Data collection was carried out at  $-60^\circ\text{C}$ .

Crystallographic data and the results of refinement are summarized in Table 3. The structural analyses were performed by Win-GX.<sup>[20]</sup> The structures of the complexes were solved by direct methods using SIR-92<sup>[21]</sup> (except **2<sup>Bu</sup>**) and SHELXS-86<sup>[22]</sup> (for **2<sup>Bu</sup>**). The structures were refined on  $F^2$  with full-matrix least-squares methods using SHELXL-97.<sup>[23]</sup> All non-hydrogen atoms, except disordered solvent molecules, were refined anisotropically.

The hydrogen atoms of the nickel-facing methyl group in **2<sup>Me</sup>** were refined isotropically. The positions of boron-attached hydrides of

Table 3. Summary of crystallographic data.

| Compound                                    | <b>1<sup>Me</sup></b>                         | <b>1<sup>Bu</sup></b>                         | <b>1<sup>H</sup>·CH<sub>2</sub>Cl<sub>2</sub></b>           | <b>1<sup>Ph</sup>·THF</b>  | <b>2<sup>Me</sup>·2EtCN</b>                                  | <b>2<sup>Bu</sup></b>  | <b>3<sup>NO3</sup>(NCMe)·2MeCN</b>                     |
|---|---|---|---|--|--|--|--|
| Formula                                     | $\text{C}_{10}\text{H}_{16}\text{BNNi}_{0.5}$ | $\text{C}_{13}\text{H}_{22}\text{BNNi}_{0.5}$ | $\text{C}_{9.25}\text{H}_{15}\text{BClN}_4\text{Ni}_{0.50}$ | $\text{C}_{17}\text{H}_{22}\text{BN}_4\text{Ni}_{0.5}\text{O}_{0.5}$ | $\text{C}_{43}\text{H}_{72}\text{B}_2\text{N}_{12}\text{Ni}$ | $\text{C}_{40}\text{H}_{68}\text{B}_2\text{N}_{10}\text{Ni}$ | $\text{C}_{33}\text{H}_{55}\text{BN}_{10}\text{NiO}_3$ |
| Formula weight                              | 232.43  | 274.51  | 257.87  | 330.55   | 837.45   | 769.37   | 709.39   |
| Crystal system                              | triclinic                                     | triclinic                                     | monoclinic  | monoclinic   | monoclinic   | orthorhombic   | monoclinic   |
| Space group                                 | $P\bar{1}$ (#2)                               | $P\bar{1}$ (#2)                               | $C2/c$ (#15)  | $P2_1/n$ (#14)   | $P2_1/c$ (#14)   | $P2_12_12_1$ (#19)   | $P2_1/n$ (#14)   |
| <i>a</i> [Å]                                | 8.195(2)                                      | 9.5021(18)                                    | 14.732(18)  | 8.393(4)   | 13.9089(10)  | 18.5584(6)   | 13.732(3)  |
| <i>b</i> [Å]                                | 9.800(2)                                      | 10.0621(6)                                    | 13.704(4)   | 15.545(3)  | 16.4183(10)  | 18.8638(6)   | 24.240(3)  |
| <i>c</i> [Å]                                | 8.0108(16)                                    | 8.1038(12)                                    | 14.033(5)   | 13.205(9)  | 21.8641(19)  | 12.7070(5)   | 12.2315(14)  |
| $\alpha$ [°]                                | 91.83(2)                                      | 101.409(13)                                   | 90.00   | 90.00  | 90.00  | 90.00  | 90.00  |
| $\beta$ [°]                                 | 93.65(2)                                      | 96.045(12)                                    | 119.833(18)   | 100.91(6)  | 96.6762(4)   | 90.00  | 98.0130(10)  |
| $\gamma$ [°]                                | 112.628(17)                                   | 103.906(5)                                    | 90.00   | 90.00  | 90.00  | 90.00  | 90.00  |
| <i>V</i> [Å <sup>3</sup> ]                  | 591.5(2)                                      | 727.67(18)                                    | 2458(3)   | 1691.8(15)   | 4959.0(6)  | 4448.5(3)  | 4031.5(11)   |
| <i>Z</i>                                    | 2   | 2   | 8   | 4  | 4  | 4  | 4  |
| <i>D</i> (calcd.) [g cm <sup>-3</sup> ]     | 1.305   | 1.253   | 1.394   | 1.298  | 1.122  | 1.149  | 1.169  |
| $\mu$ (Mo- $K_\alpha$ ) [mm <sup>-1</sup> ] | 0.844   | 0.696   | 1.030   | 0.614  | 0.432  | 0.475  | 0.524  |
| No. unique reflections                      | 2717  | 2900  | 1825  | 3197   | 10428  | 5620   | 7096   |
| No. reflections [ $I > 2\sigma(I)$ ]        | 2646  | 2595  | 1809  | 3195   | 4869   | 4231   | 5576   |
| No. parameters refined                      | 147   | 175   | 153   | 211  | 576  | 525  | 448  |
| <i>R</i> [ $I > 2\sigma(I)$ ]               | 0.0494  | 0.0451  | 0.0843  | 0.0396   | 0.0766   | 0.0420   | 0.0436   |
| <i>R</i> (for all data)                     | 0.0504  | 0.0523  | 0.0852  | 0.0400   | 0.1666   | 0.0548   | 0.0673   |
| <i>wR</i> [ $I > 2\sigma(I)$ ]              | 0.1218  | 0.1150  | 0.2286  | 0.1002   | 0.1778   | 0.1000   | 0.1271   |
| <i>wR</i> (for all data)                    | 0.1221  | 0.1171  | 0.2292  | 0.1002   | 0.2096   | 0.1042   | 0.1338   |
| GOF   | 1.173   | 1.125   | 1.108   | 1.244  | 0.970  | 0.906  | 1.102  |



$L^H$  (in  $1^H$ ) and  $Tp^{Pr2}$  (in  $2^{Me}$  and  $2^{Bu}$ ) were refined. Other hydrogen atoms [except those of the disordered solvent molecules in  $1^H \cdot CH_2Cl_2$ ,  $1^{Ph} \cdot THF$ , and  $3^{NO_3}(NCMe) \cdot 2MeCN$ , and the methine hydrogen atoms of the disordered isopropyl groups in  $2^{Me}$  and  $2^{Bu}$ ] were added in the riding model with C–H = 0.96 Å (for methyl groups), 0.98 Å (for methine groups), or 0.93 Å (for aromatic rings) with  $U_{iso}(H) = 1.2U_{iso}(\text{attached atom})$ .

CCDC-779667 ( $1^{Me}$ ), CCDC -779668 ( $1^{Bu}$ ), CCDC -779669 ( $1^H \cdot CH_2Cl_2$ ), CCDC -779670 ( $1^{Ph} \cdot THF$ ), CCDC -779671 ( $2^{Me} \cdot 2EtCN$ ), CCDC -779672 ( $2^{Bu}$ ), and CCDC -779673 [ $3^{NO_3}(NCMe) \cdot 2MeCN$ ] contain the supplementary crystallographic data for this paper. These data can be obtained free of charge from The Cambridge Crystallographic Data Centre via [www.ccdc.cam.ac.uk/data\\_request/cif](http://www.ccdc.cam.ac.uk/data_request/cif).

**Supporting Information** (see footnote on the first page of this article): Synthetic procedures and ORETP diagram of  $3^{NO_3}$  and space filling diagram of  $2^{Me}$ .

## Acknowledgments

This work was supported in part by the Grant in-Aid for Scientific Research (No. 20360367) and the Scientific Frontier Research Project from the Ministry of Education, Culture, Sports, Science, and Technology of Japan.

- [1] S. Trofimenko, *Scorpionates – The Coordination Chemistry of Polypyrazolylborate Ligands*, Imperial College Press: London, 1999.
- [2] C. Pettinari, *Scorpionates II: Chelating Borate Ligands*, Imperial College Press: London, 2008.
- [3] K. Fujita, S. Hikichi, M. Akita, Y. Moro-oka, *J. Chem. Soc., Dalton Trans.* 2000, 117–119.
- [4] K. Fujita, S. Hikichi, M. Akita, Y. Moro-oka, *J. Chem. Soc., Dalton Trans.* 2000, 1255–1260.
- [5] K. Fujita, M. Akita, S. Hikichi, *Inorg. Chim. Acta* 2009, 362, 4472–4479.
- [6] S. Hikichi, M. Kaneko, Y. Miyoshi, N. Mizuno, K. Fujita, M. Akita, *Top. Catal.* 2009, 52, 845–851.
- [7] Dimethylbis(pyridyl)borate compounds a) T. G. Hodgkins, D. R. Powell, *Inorg. Chem.* 1996, 35, 2140–2148; b) E. Khaskin, P. Y. Zavalij, A. N. Vedernikov, *J. Am. Chem. Soc.* 2006, 128, 13054–13055; c) E. Khaskin, P. Y. Zavalij, A. N. Vedernikov, *Angew. Chem. Int. Ed.* 2007, 46, 6309–6312; d) E. Khaskin, P. Y. Zavalij, A. N. Vedernikov, *J. Am. Chem. Soc.* 2008, 130, 10088–10089; e) E. Khaskin, D. L. Lew, S. Pal, A. N. Vedernikov, *Chem. Commun.* 2009, 6270–6272.
- [8] Examples of the nonpyrazolyl organoborate ligands, except imidazolyl and pyridyl compounds: see ref. 2 and the following; a) T. A. Betley, J. C. Peters, *Inorg. Chem.* 2002, 41, 6541–6543; b) C. Mazet, V. Köhler, A. Pfaltz, *Angew. Chem. Int. Ed.* 2005, 44, 4888–4891; c) V. Köhler, C. Mazet, A. Toussaint, K. Kulicke, D. Häussinger, M. Neuburger, S. Schaffner, S. Kaiser, A. Pfaltz, *Chem. Eur. J.* 2008, 14, 8530–8539; d) J. F. Dunne, J. Su, A. Ellern, A. D. Sadow, *Organometallics* 2008, 27, 2399–2401; e) B. Baird, A. V. Pawlikowski, J. Su, J. W. Wiench, M. Pruski, A. D. Sadow, *Inorg. Chem.* 2008, 47, 10208–10210; f) A. V. Pawlikowski, A. Ellern, A. D. Sadow, *Inorg. Chem.* 2009, 48, 8020–8029; g) J. F. Dunne, K. Manna, J. W. Wiench, A. Ellern, M. Pruski, A. D. Sadow, *Dalton Trans.* 2010, 39, 641–653; h) A. A. Barney, A. F. Heyduk, D. G. Nocera, *Chem. Commun.* 1999, 2379–2380; i) J. C. Thomas, J. C. Peters, *J. Am. Chem. Soc.* 2001, 123, 5100–5101; j) P. Ge, B. S. Haggerty, A. L. Rheingold, C. G. Riordan, *J. Am. Chem. Soc.* 1994, 116, 8406–8407; k) C. Ohrenberg, P. Ge, P. Schebler, C. G. Riordan, G. P. A. Yap, A. L. Rheingold, *Inorg. Chem.* 1996, 35, 749–754; l) C. Ohrenberg, L. M. Liable-Sands, A. L. Rheingold, C. G. Riordan, *Inorg. Chem.* 2001, 40, 4276–4283.
- [9] W. H. Glaze, G. M. Adams, *J. Am. Chem. Soc.* 1966, 88, 4653–4656 and references cited therein.
- [10] a) S. Trofimenko, *J. Am. Chem. Soc.* 1967, 89, 6288–6294; b) H. M. Echols, D. Dennis, *Acta Crystallogr., Sect. B* 1974, 30, 2173–2176; c) H. M. Echols, D. Dennis, *Acta Crystallogr., Sect. B* 1976, 32, 1627–1630; d) D. A. Clemente, M. Cingi-Biagini, *Inorg. Chem.* 1987, 26, 2350–2359; e) F. A. Cotton, C. A. Murillo, *Inorg. Chim. Acta* 1976, 17, 121–124; f) H. Kokusen, Y. Sohrin, M. Matsui, Y. Hata, H. Hasegawa, *J. Chem. Soc., Dalton Trans.* 1996, 195–201.
- [11] See for example: a) P. G. Gjhosh, J. B. Bonanno, G. Parkin, *J. Chem. Soc., Dalton Trans.* 1998, 2779–2781; b) J. C. Calabrese, P. J. Domaille, J. S. Thompson, S. Trofimenko, *Inorg. Chem.* 1990, 29, 4429–4437.
- [12] a) S. Trofimenko, *J. Am. Chem. Soc.* 1968, 90, 4754–4755; b) S. Trofimenko, *Inorg. Chem.* 1970, 9, 2493–2499; c) F. A. Cotton, T. LaCour, A. G. Stanislawski, *J. Am. Chem. Soc.* 1974, 96, 754–760; d) F. A. Cotton, T. LaCour, A. G. Stanislawski, *J. Am. Chem. Soc.* 1974, 96, 5074–5082; e) F. A. Cotton, V. W. Day, *J. Chem. Soc., Chem. Commun.* 1974, 415–416; f) F. A. Cotton, *Inorg. Chem.* 2002, 41, 643–658.
- [13] a) S. Trofimenko, J. C. Calabrese, J. S. Thompson, *Angew. Chem. Int. Ed. Engl.* 1989, 28, 205–206; b) S. Trofimenko, J. C. Calabrese, J. S. Thompson, *Inorg. Chem.* 1992, 31, 974–979.
- [14] Reviews: a) M. Brookhart, M. L. H. Green, G. Parkin, *Proc. Natl. Acad. Sci. USA* 2007, 104, 6908–6914; b) M. Etienne, J. E. McGrady, F. Maseras, *Coord. Chem. Rev.* 2009, 253, 635–646; c) W. Scherer, G. S. McGrady, *Angew. Chem.* 2004, 116, 1816–1842; *Angew. Chem. Int. Ed.* 2004, 43, 1782–1806.
- [15] a) W. I. Sundquist, D. P. Bancroft, S. J. Lippard, *J. Am. Chem. Soc.* 1990, 112, 1590–1596; b) Y. Zhang, J. C. Lewis, R. G. Bergman, J. A. Ellman, E. Oldfield, *Organometallics* 2006, 25, 3515–3519; c) A. Mukhopadhyay, S. Pal, *Eur. J. Inorg. Chem.* 2006, 4879–4887.
- [16] N. Kitajima, S. Hikichi, M. Tanaka, Y. Moro-oka, *J. Am. Chem. Soc.* 1993, 115, 5496–5508.
- [17] The molecular structure of an analogous cobalt(II)-nitrate complex has been reported: U. P. Singh, P. Babbar, A. K. Sharma, *Inorg. Chim. Acta* 2005, 358, 271–278.
- [18] D. D. Perrin, W. L. Armarego, D. R. Perrin, *Purification of Laboratory Chemicals*, 2nd ed., Pergamon, New York, 1980.
- [19] H. Kanai, K. Kushi, K. Sakanoue, N. Kishimoto, *Bull. Chem. Soc. Jpn.* 1980, 53, 2711–2715.
- [20] L. J. Farrugia, *J. Appl. Crystallogr.* 1999, 32, 837–838.
- [21] A. Altomare, M. C. Burla, M. Camalli, M. Cascarano, C. Giacovazzo, A. Guagliardi, G. Polidori, *J. Appl. Crystallogr.* 1994, 27, 435–436.
- [22] G. M. Sheldrick, *SHELXS-86*, University of Göttingen, Göttingen, Germany, 1986.
- [23] a) G. M. Sheldrick, *SHELXL-97*, University of Göttingen, Germany, 1997; b) G. M. Sheldrick, *Acta Crystallogr., Sect. A* 2008, 64, 112–122.

Received: June 5, 2010

Published Online: October 29, 2010